LAWRENCE
LIVERMORE
NATIONAL
LABORATORY

UCRL-PROC-220305

Anodic Behavior of Alloy 22 in High Nitrate Brines at Temperatures Higher than 100(degree)C

G. O. Ilevbare, R. A. Etien, J. C. Estill, G. A. Hust, A. Yilmaz, M. L. Stuart, R. B. Rebak

March 31, 2006

2006 ASME Pressure Vessels and Piping Division Conference
Vancouver, Canada
July 23, 2006 through July 27, 2006

Proceedings of PVP2006
2006 ASME Pressure Vessels and Piping Division Conference
July 23-27, 2006, Vancouver, British Columbia, Canada
PVP2006-ICPVT11-93423

ANODIC BEHAVIOR OF ALLOY 22 IN HIGH NITRATE BRINES AT TEMPERATURES HIGHER THAN 100°C

Gabriel O. Ilevbare[1] **Robert A. Etien[2]**

John C. Estill **Gary A. Hust**

Ahmet Yilmaz[3] **Marshall L. Stuart**

Raul B. Rebak

Lawrence Livermore National Laboratory
7000 East Ave, L-631
Livermore, California, 94550 USA
[1] Currently with Integrated Science Solutions Inc., Walnut Creek, CA
[2] Currently with Knolls Atomic Power Laboratory, Schenectady, NY
[3] Currently with AMRDEC/Westar, Redstone Arsenal, AL

ABSTRACT

Alloy 22 (N06022) may be susceptible to crevice corrosion in chloride solutions. Nitrate acts as an inhibitor to crevice corrosion. Several papers have been published regarding the effect of nitrate on the corrosion resistance of Alloy 22 at temperatures 100°C and lower. However, very little is known about the behavior of this alloy in highly concentrated brines at temperatures above 100°C. In the current work, electrochemical tests have been carried out to explore the anodic behavior of Alloy 22 in high chloride high nitrate electrolytes at temperatures as high as 160°C at ambient atmospheres. Even though Alloy 22 may adopt corrosion potentials in the order of +0.5 V (in the saturated silver chloride scale), it does not suffer crevice corrosion if there is high nitrate in the solution. That is, the inhibitive effect of nitrate on crevice corrosion is active for temperatures higher than 100°C.

Keywords: N06022, Calcium Chloride, High Nitrate, High Temperature, Corrosion Potential, Corrosion Rate

INTRODUCTION

Alloy 22 (N06022) is a nickel base alloy designed to be resistant to all forms of corrosion. Alloy 22 (N06022) contains approximately 56% nickel (Ni), 22% chromium (Cr), 13% molybdenum (Mo), 3% tungsten (W) and 3% iron (Fe) (ASTM B 575). [1] Because of its high level of Cr, Alloy 22 remains passive in most industrial environments and therefore has an exceptionally low general corrosion rate. [2-6] The combined presence of Cr, Mo and W imparts Alloy 22 with high resistance to localized corrosion such as pitting corrosion and stress corrosion cracking even in hot high chloride (Cl^-) solutions. [7-12] It has been reported that Alloy 22 may suffer localized corrosion such as crevice corrosion when it is anodically polarized in chloride containing solutions. [8-10,13-15] It is also known that the presence of nitrate (NO_3^-) and other oxyanions in the solution minimizes or eliminates the susceptibility of Alloy 22 to crevice corrosion. [8-10,16-23] The value of the ratio ($[NO_3^-]/([Cl^-]$) has a strong effect of the susceptibility of Alloy 22 to crevice corrosion. [16-23] The higher the nitrate to chloride ratio the stronger the inhibition by nitrate.

From the general and localized corrosion point of view, it is important to know the value of E_{corr} for Alloy 22 under different environmental conditions. [18] The corrosion degradation model for the Yucca Mountain nuclear waste container assumes that localized corrosion will only occur when E_{corr} is equal or greater than a critical potential (E_{crit}) for the onset of localized corrosion. [18] That is, if $E_{corr} < E_{crit}$ or $\Delta E = E_{crit} - E_{corr} > 0$, general or passive corrosion will occur and localized corrosion is not expected. Passive corrosion rates of Alloy 22 are generally exceptionally low. In environments that promote localized corrosion, E_{crit} is the lowest potential that would initiate crevice corrosion. The value of E_{crit} is generally

ascribed as the repassivation potential for crevice corrosion obtained using the cyclic potentiodynamic polarization (CPP) curve described in ASTM G 61. [18] From the CPP, the repassivation potential is taken as the potential at which the reverse-scan line crosses over the forward scan. This potential is called the repassivation potential cross-over (ERCO). By knowing the values of E_{corr} and E_{crit} (or ERCO) of Alloy 22, the likelihood or necessary conditions for the alloy to suffer crevice corrosion under natural polarization (e.g. oxygen from air) can be established.

All the previously published work mainly concentrated on the behavior of Alloy 22 at temperatures approximately 100°C and below. Highly soluble salts such as potassium nitrate can produce concentrated solutions that will remain liquid to temperatures higher than 150°C at ambient pressure. [24] The purpose of the current work was to examine the corrosion behavior of Alloy 22 in highly concentrated brines at temperatures 100°C and higher.

EXPERIMENTAL TECHNIQUE

Different types of Alloy 22 (N06022) specimens were used to assess corrosion potential (E_{corr}), corrosion rate (CR) and the crevice corrosion resistance as a function of chloride concentration, nitrate over chloride ratio, temperature and immersion time. Both welded and non-welded specimens were used. Creviced specimens were machined from welded 1.25-inch thick plates (~32 mm). Table 1 shows the chemical composition of the heats for the base plate and the welding wire. The plates were welded using the gas tungsten arc welding (GTAW) technique from both sides of the plate using the double V groove technique. The specimens were in the form of multiple crevice assemblies (MCA) (Figure 1), prism crevice assemblies (PCA) (Figure 2) and rods. The exposed surface area for each type of specimen was different. The 0.25-inch diameter MA rods were immersed 2-inches deep into the electrolyte and the exposed surface area was 5.4 cm². The ASW and ASW + HTA rods were immersed 0.5-inch deep and the surface area was 2.9 cm². The area of the MCA specimens was 7.4 cm² for the cyclic polarization. The area under the crevice was included. The PCA specimens were fully immersed and the area was 14.06 cm². The surface area of the PCA did not include the area covered by the crevice formers (CF), which was approximately 1.5 cm². The PCA had a mounting mechanism for the connecting rod explained in ASTM G 5 (Figure 1). [25] The crevice formers were mounted on both sides of the specimen. Each crevice former consisted of a washer made of a ceramic material containing 12 crevicing spots or teeth with gaps in between the teeth (ASTM G 48). [25] Before mounting them onto the metallic specimens, the CF were covered with PTFE tape to ensure a tight crevicing gap between the CF and the specimens. The specimens had a ground surface finish of 600-grit paper. For the long-term monitoring of E_{corr} and CR, there were two types of welded MCA specimens: (1) The as-welded (ASW) which were as-received welded specimens and (2) the as-welded plus solution annealed or solution heat treated (ASW + SHT) plus water quenched. After this high-temperature treatment the SHT specimens were left with the black annealed oxide film on the surface.

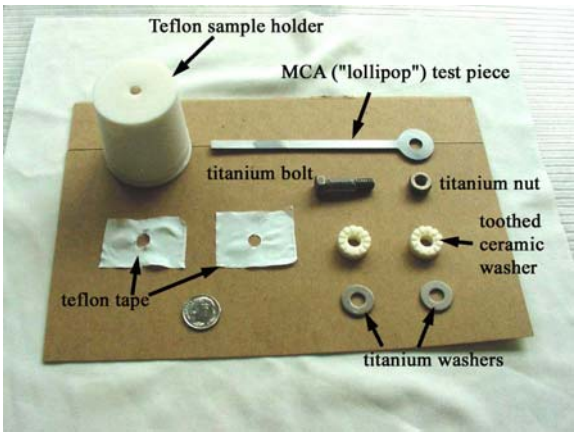

Figure 1. MCA Specimen and hardware

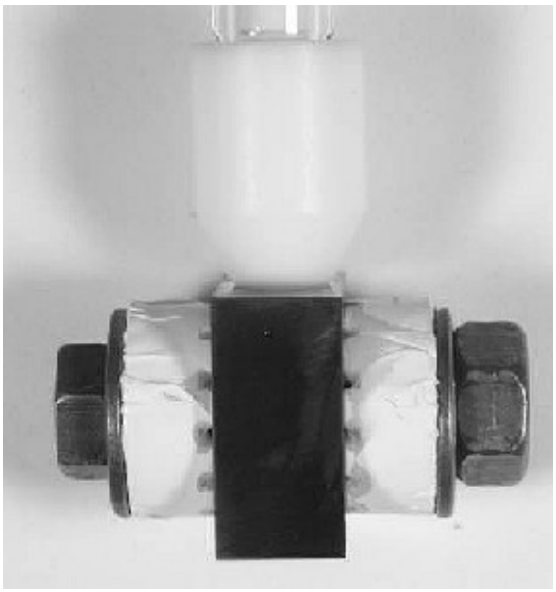

Figure 2. Assembled PCA Specimen

Three different sets of electrochemical tests were performed: (1) Monitoring of the corrosion potential and corrosion rate as a function of time, (2) Cyclic Potentiodynamic Polarization (CPP) (ASTM G 61) [25] and (3) Potentiostatic tests.

During the long-term monitoring of E_{corr}, pure platinum rods (ASTM B 561) [1] were also used for testing. The platinum

rods were 1/8-inch in diameter and 12-inch long. The rods were immersed 1-inch deep into the electrolyte solutions.

Several types of electrolytes were used, from pure $CaCl_2$ solutions to solutions containing high concentration of nitrate. Table 2 shows a list of tested electrolytes and tested temperatures. For the constant potential and cyclic polarization tests the electrolytes were deaerated with purified nitrogen and for the long-term corrosion potential monitoring the electrolytes were naturally aerated (air was circulated above the solution but it was not purged through the solution). The gas stream (N_2 or air) exited the vessel through a condenser to avoid evaporation of the electrolyte. The volume of the electrolyte solutions was 2 liters (2 L) for the E_{corr} monitoring and 900 cc for the constant potential and cyclic polarization tests. Potentials were monitored using saturated silver chloride electrodes [SSC] through a Luggin capillary. The reference electrode was kept near room temperature using a jacketed electrode holder through which cooled water was re-circulated. The potentials in this paper are reported in the saturated silver chloride scale [SSC]. At ambient temperature, the SSC scale is 199 mV more positive than the normal hydrogen electrode (NHE).

The value of the free corrosion potentials or open circuit potentials were acquired using a commercial data acquisition (DA) unit that had the input resistance set at 10 G-ohm. Typically, the measurements were acquired every minute for the first day and every hour after the first day. The data was logged into in the internal memory of the DA unit and simultaneously to a spreadsheet in an interfaced personal computer. Usually, data back up was performed monthly. Corrosion rates were calculated both for 24-h immersion tests (just before performing the cyclic polarization tests) and for the long-term immersion in aerated electrolytes. The corrosion rates were calculated using the polarization resistance (PR) technique (ASTM G 59). [25] The polarization resistance values ($\Omega.cm^2$) were later converted to corrosion rates (μm/year). To measure the polarization resistance, an initial potential of 20 mV below the corrosion potential (E_{corr}) was ramped to a final potential of 20 mV above E_{corr} at a rate of 0.167 mV/s. Linear fits were constrained to the potential range of 10 mV below E_{corr} to 10 mV above E_{corr}. In a plot potential vs. current the slope is defined as R_p or resistance to polarization (ASTM G 59). To calculate R_p, the potential was plotted in the X-axis and the current (dependent variable) in the Y-axis. The Tafel constants, b_a and b_c, were assumed to be ±0.120 V/decade. Corrosion rates were calculated using Equations 1 and 2

$$i_{corr} = \frac{1}{R_p} \cdot \frac{b_a \cdot b_c}{2.303(b_a + b_c)} \qquad (1)$$

$$CR(\mu m / yr) = k \frac{i_{corr}}{\rho} EW \qquad (2)$$

Where k is a conversion factor (3.27×10^6 $\mu m \cdot g \cdot A^{-1} \cdot cm^{-1} \cdot yr^{-1}$), i_{corr} is the corrosion current density in A/cm², which is calculated from resistance to polarization (R_p) slopes (Eq. 1), EW is the equivalent weight of Alloy 22 (23.28), and ρ is the density of Alloy 22 (8.69 g/cm³). The EW was calculated assuming an equivalent dissolution of the major alloying elements as Ni^{2+}, Cr^{3+}, Mo^{6+}, Fe^{2+}, and W^{6+} (ASTM G 102). [25]

EXPERIMENTAL RESULTS AND DISCUSSION

Evolution of the Corrosion Potential and the Corrosion Rate

Figure 3 shows the evolution of the E_{corr} for three Alloy 22 specimens as a function of the immersion time in naturally aerated 18 m $CaCl_2$ + 9 m $Ca(NO_3)_2$ solution at 155°C. The reading of the E_{corr} was generally done monthly. More detailed (every hour) readings still need to be analyzed. Figure 3 shows that the E_{corr} for the three types of specimens was high, i.e. near the region of transpassivity of chromium. The E_{corr} slightly decreased as the time increased. The E_{corr} for the rod and the creviced specimens was practically the same (Fig. 3). Also the E_{corr} of as-welded polished PCA specimen was the same as the PCA specimen containing the black annealed film on the surface (Fig. 3). This is an on-going test, that is, examination of the corroded specimens is not possible at this time.

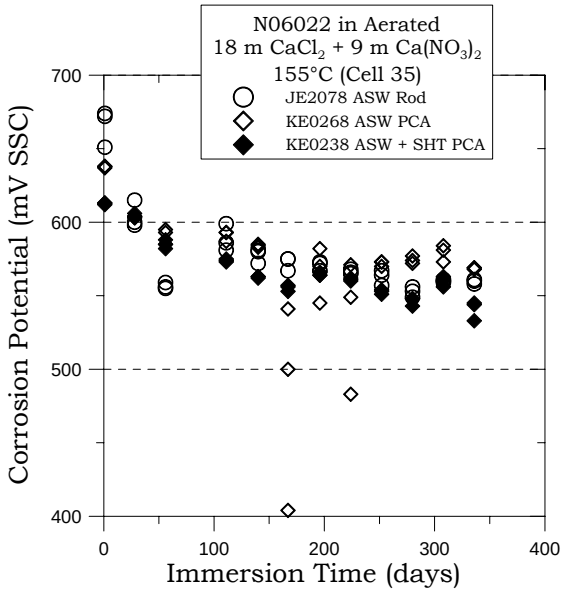

Figure 3. Monthly E_{corr} of Rod and PCA of Welded Alloy 22 in 18 m $CaCl_2$ + 9 m $Ca(NO_3)_2$ at 155°C

Figure 4 shows the evolution of the corrosion rate of welded Alloy 22 specimens in the same environment as in Fig. 3. Figure 4 shows that the corrosion rate for the PCA specimen containing the black annealed oxide film on the surface was

approximately constant with time and in the order of 0.1-0.3 µm/year. The corrosion rate of the freshly polished specimens (open symbols in Fig. 4) seemed to have slightly increased as the time increased. However, their corrosion rates were nonetheless low and in the order of only 1-2 µm/year after a year of immersion in the concentrated electrolyte.

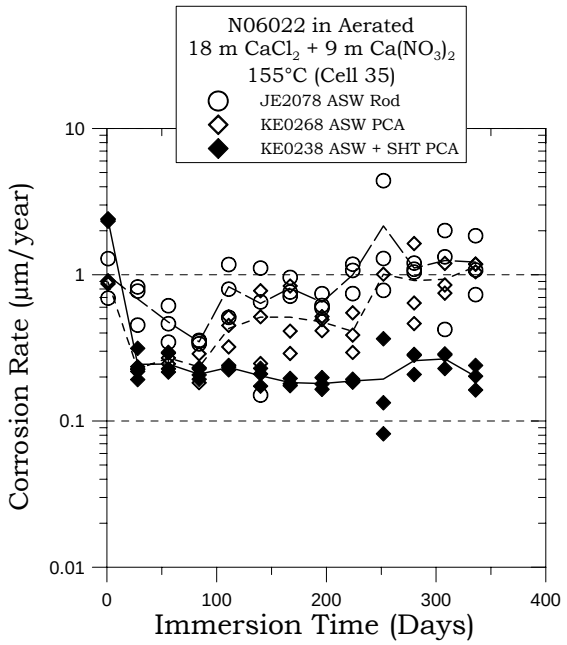

Figure 4. Monthly Corrosion Rate of Rod and PCA of Welded Alloy 22 in 18 m $CaCl_2$ + 9 m $Ca(NO_3)_2$ at 155°C

Effect of Solution Composition on the Short-Term Corrosion Rate

Figure 5 shows the corrosion rate of Alloy 22 creviced MCA specimens after 24-h immersion in deaerated 10-18 m $CaCl_2$ brines containing $Ca(NO_3)_2$ to reach ratios of nitrate over chloride of 0, 0.05, 0.15 and 0.5. In the nitrate-free solution ($[NO_3^-]/[Cl^-]$ = 0), as the temperature (and chloride concentration) increased, the corrosion rate increased. Also, at each temperature, and for each base $CaCl_2$ concentration, as the ratio of $[NO_3^-]/[Cl^-]$ increased the corrosion rate decreased. Figure 5 shows that the presence of nitrate in the electrolyte not only inhibits crevice corrosion (see following sections) but also reduces the general corrosion rate of the alloy. In the $[NO_3^-]/[Cl^-]$ = 0.5 solutions, the corrosion rate was in the order of 1 µm/year or lower for all the three tested chloride concentrations. The data in Figure 5 are for short-immersion times and are not intended to represent the long-term corrosion behavior of Alloy 22 in the given electrolyte solutions.

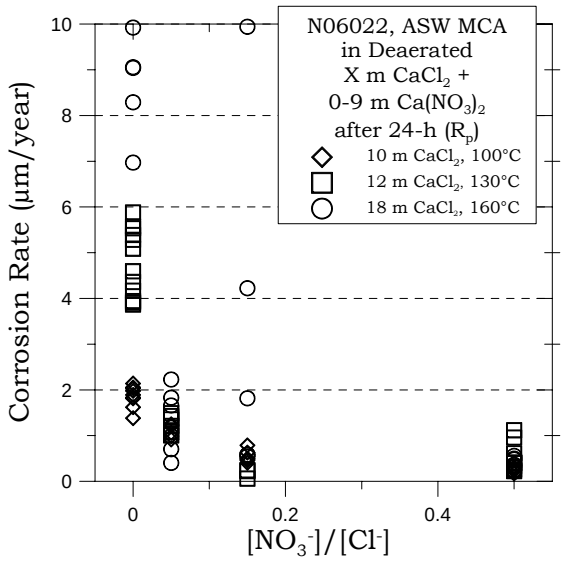

Figure 5. 24-h Immersion Corrosion Rate of Alloy 22. Effect of Solution Composition

Anodic Behavior During Cyclic Polarization

Figure 6 shows the anodic behavior of Alloy 22 at 130°C in 12 m $CaCl_2$ solutions containing different amounts of nitrate.

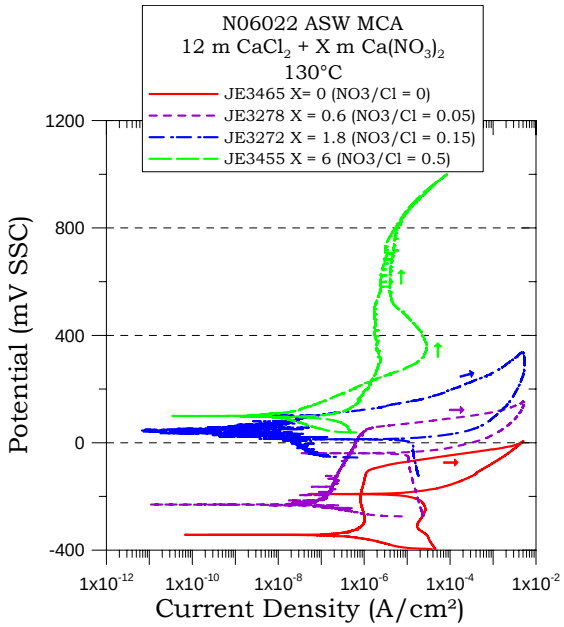

Figure 6. Cyclic Polarization of Alloy 22 in 12 m $CaCl_2$ solutions at 130°C.

In the nitrate-free solution, the breakdown potential is below 0 V (SSC) (Fig. 6). A small addition of 0.6 m $Ca(NO_3)_2$ increased the breakdown potential to above 0 V and reduced

the passive current density. For the nitrate free solution and for the $[NO_3^-]/[Cl^-]$ = 0.05 and 0.15 solutions, the anodic polarization curves showed a hysteresis in the reverse scan suggesting the presence of localized corrosion after passivity breakdown. For the $[NO_3^-]/[Cl^-]$ = 0.5 solution, Alloy 22 did not suffer breakdown of passivity even for anodic polarization values in the order of 1 V. Also, the reverse scan did not show hysteresis (Fig. 6).

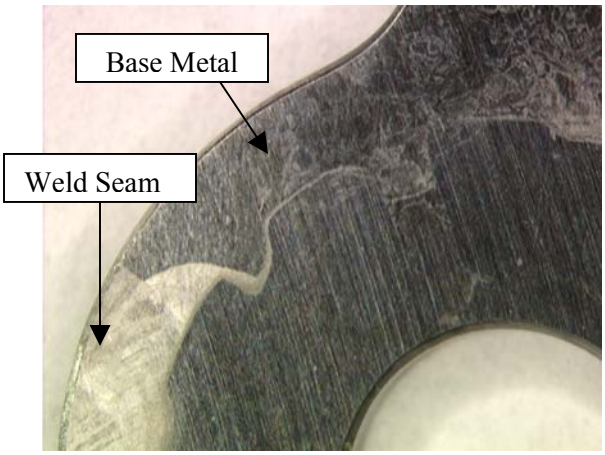

Figure 7. Specimen JE3461 After CPP in 18 m $CaCl_2$ at 160°C. Massive Attack Outside Crevice Formers

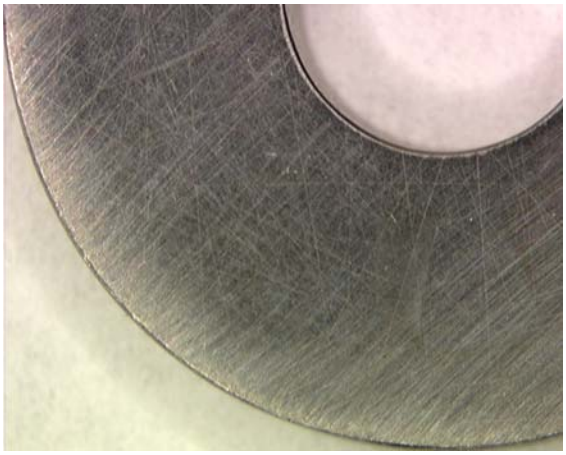

Figure 8. Specimen JE3281 After CPP in 18 m $CaCl_2$ + 9 m $Ca(NO_3)_2$ at 160°C
No Discernible Attack - Nitrate Inhibition

Figures 7 and 8 show the appearance of the tested specimens after the cyclic potentiodynamic polarization (CPP) testing and the effect of the addition of nitrate to the chloride solution. In the nitrate-free environments at 160°C, $CaCl_2$ produced a massive attack to the specimen outside the crevice formers (Figure 7). When smaller amounts of nitrate were added (e.g. $[NO_3^-]/[Cl^-]$ = 0.05) the area of attack diminished and when the ratio $[NO_3^-]/[Cl^-]$ was 0.5, the localized attack on the specimen was suppressed (Figure 8). Figure 9 shows the appearance of a specimen tested in a solution at 145°C containing $[NO_3^-]/[Cl^-]$ = 100 (Table 2). These results show that high nitrate solutions inhibit the localized corrosion in Alloy 22 even at temperatures in the order of 150°C.

Figure 9. Specimen JE3297 After CPP in 0.225 m $MgCl_2$ + 22.5 m $Ca(NO_3)_2$ at 145°C
No Discernible Corrosion Attack

Table 2 shows parameters from the CPP tests. These parameters can be separated as: (1) Short-Term Corrosion Potential (E_{corr}), (2) Breakdown Potentials (E20 and E200) and (3) Repassivation Potentials (ER10, ER1 and ERCO). See Table 2 for explanations. The effect of temperature and nitrate concentration can be assessed by comparison of these parameters. For example, in the 12 m $CaCl_2$ solution at 130°C the average breakdown potential E20 was –48 mV SSC but when nitrate is added to the solution to ratios over chloride of 0.05, 0.15 and 0.5, the E20 value continuously increased to average values of 62, 184 and 759 mV SSC (Table 2).

Constant Potential Tests

Table 3 shows the matrix of the constant potential or potentiostatic tests. Figure 10 shows two potentiostatic tests performed in the concentrated solution of 0.225 m $MgCl_2$ + 22.5 m $Ca(NO_3)_2$ at 145°C. In spite of the high applied potential, the current remained steady for the duration of the tests (Fig. 10). After the tests the specimens were free from localized corrosion and only transpassive dissolution occurred (Fig. 11). The area of the specimen covered by the crevice formers was free from corrosion. Table 3 shows the results of the other constant potential tests. If attack occurred at the applied potentials in high nitrate solutions, it was in the form of transpassivity or localized corrosion outside the footprints of

the crevice formers. This localized corrosion manifested itself as a superficial worm-in-wood type of attack. Crevice corrosion did not occur.

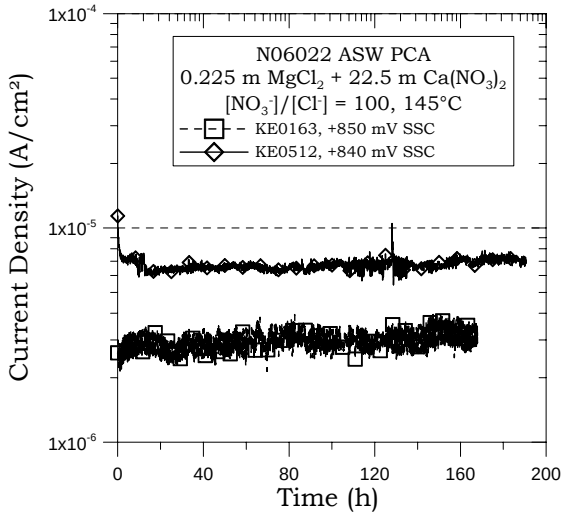

Figure 10. Potentiostatic Tests in High Nitrate Solution

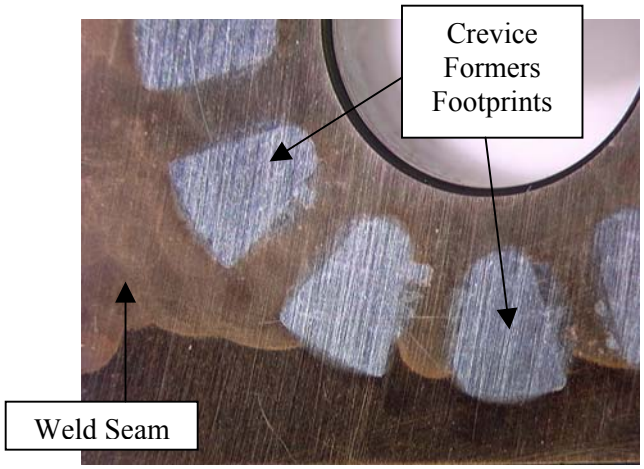

Figure 11. Specimen KE0163 after Potentiostatic Test in High Nitrate Solution

Concluding Remarks

More research is needed in the area of high temperature highly concentrated solutions. It appears that, when localized corrosion occurs, the mode of attack shifts from mainly crevice corrosion at temperatures below 100°C to an uneven surface attack outside the crevice formers at temperatures higher than approximately 120°C. The type of attack may also be associated to the mode the current is applied to the specimen. That is, if the current is applied in a continuous potential scanning such as in the CPP tests, the mode of attack may appear different than if the current is applied in a galvanostatic mode, for example. Results discussed briefly here are for concentrated brines based in the Ca system. More recent research is focused in the Na and K system. [24] Currently localized corrosion and boiling point of solution studies are being focused in the NaCl, KNO_3 and $NaNO_3$ systems. These systems may better represent conditions of dust deliquescence.

CONCLUSIONS

(1) Nitrate is an inhibitor for both localized corrosion and general corrosion

(2) The inhibitive effect of nitrate is valid also at temperatures higher than 100°C

(3) In high nitrate brines the E_{corr} of Alloy 22 remains high (~0.5 V SCC) even after a year of monitoring

(4) Constant potential tests in high nitrate brines showed transpassive dissolution due to the high potentials applied but did not show localized corrosion

ACKNOWLEDGMENTS

The authors gratefully acknowledge the participation of Steven R. Gordon in some of the tests. This work was performed under the auspices of the U. S. Department of Energy by the University of California Lawrence Livermore National Laboratory under contract No. W-7405-Eng-48. This work is supported by the Yucca Mountain Project, which is part of the DOE Office of Civilian Radioactive Waste Management (OCRWM)

REFERENCES

1. ASTM International, Volume 02.04, Standard B 575 (ASTM International, 2003: West Conshohocken, PA).
2. Haynes International, "Hastelloy C-22 Alloy", Brochure H-2019E (Haynes International, 1997: Kokomo, IN).
3. R. B. Rebak in Corrosion and Environmental Degradation, Volume II, p. 69, Wiley-VCH, Weinheim, Germany (2000).
4. R. B. Rebak and P. Crook, "Nickel Alloys for Corrosive Environments," Advanced Mater. & Proc., 157, 37, 2000

5. R. B. Rebak and P. Crook "Influence of the Environment on the General Corrosion Rate of Alloy 22," PVP-Vol 483 pp. 131-136 (ASME, 2004: New York, NY).
6. R. B. Rebak and Joe H. Payer, "Passive Corrosion Behavior of Alloy 22," ANS Conf. International High Level Radioactive Waste Management, Las Vegas 30Apr-04May 2006.
7. R. B. Rebak and P. Crook "Improved Pitting and Crevice Corrosion Resistance of Nickel and Cobalt Based Alloys," ECPV 98-17, pp. 289-302 (The Electrochemical Society, 1999: Pennington York, NJ).
8. B. A. Kehler, G. O. Ilevbare and J. R. Scully, Corrosion, 1042 (2001).
9. K. J. Evans and R. B. Rebak in Corrosion Science – A Retrospective and Current Status in Honor of Robert P. Frankenthal, PV 2002-13, p. 344-354 (The Electrochemical Society, 2002: Pennington, NJ).
10. K. J. Evans, S. D. Day, G. O. Ilevbare, M. T. Whalen, K. J. King, G. A. Hust, L. L. Wong, J. C. Estill and R. B. Rebak, PVP-Vol. 467, Transportation, Storage and Disposal of Radioactive Materials – 2003, p. 55 (ASME, 2003: New York, NY).
11. Y-M. Pan, D. S. Dunn and G. A. Cragnolino in Environmentally Assisted Cracking: Predictive Methods for Risk Assessment and Evaluation of Materials, Equipment and Structures, STP 1401, pp. 273-288 (West Conshohocken, PA: ASTM 2000).
12. R. B. Rebak in Environmentally Assisted Cracking: Predictive Methods for Risk Assessment and Evaluation of Materials, Equipment and Structures, STP 1401, pp. 289-300 (West Conshohocken, PA: ASTM 2000).
13. C. S. Brossia, L. Browning, D. S. Dunn, O. C. Moghissi, O. Pensado and L. Yang "Effect of Environment on the Corrosion of Waste Package and Drip Shield Materials," Publication of the Center for Nuclear Waste Regulatory Analyses (CNWRA 2001-03), September 2001.
14. D. S. Dunn, L. Yang, Y.-M. Pan and G. A. Cragnolino "Localized Corrosion Susceptibility of Alloy 22," Paper 03697 (NACE International, 2003: Houston, TX).
15. K. J. Evans, A. Yilmaz, S. D. Day, L. L. Wong, J. C. Estill and R. B. Rebak "Comparison of Electrochemical Methods to Determine Crevice Corrosion Repassivation Potential of Alloy 22 in Chloride Solutions," JOM, p. 56, January 2005.
16. G. A. Cragnolino, D. S. Dunn and Y.-M. Pan "Localized Corrosion Susceptibility of Alloy 22 as a Waste Package Container Material," Scientific Basis for Nuclear Waste Management XXV, Vol. 713 (Materials Research Society 2002: Warrendale, PA).
17. D. S. Dunn and C. S. Brossia "Assessment of Passive and Localized Corrosion Processes for Alloy 22 as a High-Level Nuclear Waste Container Material," Paper 02548 (NACE International, 2002: Houston, TX).
18. J. H. Lee, T. Summers and R. B. Rebak "A Performance Assessment Model for Localized Corrosion Susceptibility of Alloy 22 in Chloride Containing Brines for High Level Nuclear Waste Disposal Container," Paper 04692 (NACE International, 2004: Houston, TX).
19. D. S. Dunn, L. Yang, C. Wu and G. A. Cragnolino, Material Research Society Symposium, Spring 2004, San Francisco, Proc. Vol 824 (MRS, 2004: Warrendale, PA)
20. D. S. Dunn, Y.-M. Pan, L. Yang and G. A Cragnolino and X. He "Localized Corrosion Resistance and Mechanical Properties of Alloy 22 Waste Package Outer Containers" JOM, January 2005, pp 49-55.
21. R. B. Rebak, "Factors Affecting the Crevice Corrosion Susceptibility of Alloy 22," Paper 05610, Corrosion/2005 (NACE International, 2005: Houston, TX)
22. D. S. Dunn, Y.-M. Pan, L. Yang and G. A Cragnolino, Corrosion, 61, 11, 1076, 2005
23. G. O. Ilevbare, K. J. King, S. R. Gordon, H. A. Elayat, G. E. Gdowski and T. S. E. Summers, Journal of The Electrochemical Society, 152, 12, B547-B554, 2005
24. J. Rard, K. Staggs, S. D. Day and S. A. Carroll, "Boiling Temperature and Reversed Deliquescence Relative Humidity Measurements for Mineral Assemblages in the $NaCl+NaNO_3+KNO_3+Ca(NO_3)_2+H_2O$ System" J. Solution Chemistry (accepted for publication)
25. ASTM International, Volume 03.02, Standards G 5, G 48, G 59, G 61, G 102 (ASTM International, 2003: West Conshohocken, PA).

Table 1. Heats and Approximate Composition of N06022 Specimens

Specimens	Heat - Manufacturer	Approximate Composition
ASW PCA KE0151 to KE0239 ASW PCA KE0351 to KE0400 ASW PCA KE0401 to KE0700 ASW MCA JE3451 to JE3470	Base Plate by Haynes International Heat 2277-0-3183 Weld Wire by Inco Alloys Heat XX1829BG	Base Metal = 55.29 Ni, 21.23 Cr, 13.37 Mo, 2.93 W, 3.65 Fe, 1.7 Co, 0.23 Mn, 0.14 V, Filler Metal = 59.31 Ni, 20.44 Cr, 14.16 Mo, 3.07 W, 2.2 Fe, 0.21 Mn, 0.15 Cu
ASW MCA JE3201 to JE3239	Base Plate by Jessop, Heat 059902LL1 Weld Wire by Inco Alloys Heat XX1829BG	Base Metal = 59.56 Ni, 20.38 Cr, 13.82 Mo, 2.64 W, 2.85 Fe, 0.16 Mn, 0.17 V, Filler Metal = See above
ASW MCA JE3240 to JE3300 ASW PCA KE0101 to KE0150	Base Plate by Jessop, Heat 059902LL2 Weld Wire by Inco Alloys Heat XX2048BG	Base Metal = 59.56 Ni, 20.38 Cr, 13.82 Mo, 2.64 W, 2.85 Fe, 0.16 Mn, 0.17 V, Filler Metal = 59.4 Ni, 20.48 Cr, 14.21 Mo, 3.02 W, 2.53 Fe, 0.2 Mn

Table 2. Tested Conditions and Characteristic Potentials (mV, SSC) from the Cyclic Polarization Curves (CPP)

Specimen ID	Type of Specimen	Solution	Temp. (°C)	$[NO_3^-]/[Cl^-]$	E20	E200	ER10	ER1	ERCO
JE3457	ASW MCA	10 m $CaCl_2$	100	0	23	37	NA	NA	NA
JE3458	ASW MCA	10 m $CaCl_2$	100	0	-2	16	NA	NA	NA
JE3463	ASW MCA	10 m $CaCl_2$	100	0	-24	8	-167	-194	-197
JE3464	ASW MCA	10 m $CaCl_2$	100	0	60	70	-157	-181	-183
JE3270	ASW MCA	10 m $CaCl_2$ + 0.5 m $Ca(NO_3)_2$	100	0.05	72	143	-30	-38	-39
JE3284	ASW MCA	10 m $CaCl_2$ + 0.5 m $Ca(NO_3)_2$	100	0.05	29	133	-35	-42	-41
JE3276	ASW MCA	10 m $CaCl_2$ + 1.5 m $Ca(NO_3)_2$	100	0.15	176	190	28	15	NA
JE3285	ASW MCA	10 m $CaCl_2$ + 1.5 m $Ca(NO_3)_2$	100	0.15	79	142	23	9	18
JE3286	ASW MCA	10 m $CaCl_2$ + 5 m $Ca(NO_3)_2$	100	0.5	165	275	121	89	105
JE3287	ASW MCA	10 m $CaCl_2$ + 5 m $Ca(NO_3)_2$	100	0.5	208	305	934	694	NA
KE0369	ASW PCA	10 m $CaCl_2$ + 5 m $Ca(NO_3)_2$	100	0.5	238			81	76
KE0370	ASW PCA	10 m $CaCl_2$ + 5 m $Ca(NO_3)_2$	100	0.5	252			96	87
KE0371	ASW PCA	10 m $CaCl_2$ + 5 m $Ca(NO_3)_2$	100	0.5	247			85	83
KE0372	ASW PCA	10 m $CaCl_2$ + 5 m $Ca(NO_3)_2$	100	0.5	320			196	179
JE3459	ASW MCA	12 m $CaCl_2$	130	0	-46	-27	NA	NA	NA
JE3460	ASW MCA	12 m $CaCl_2$	130	0	-28	-2	NA	NA	NA
JE3465	ASW MCA	12 m $CaCl_2$	130	0	-63	-40	-185	-190	-190
JE3466	ASW MCA	12 m $CaCl_2$	130	0	-55	-33	-184	-191	-191
JE3271	ASW MCA	12 m $CaCl_2$ + 0.6 m $Ca(NO_3)_2$	130	0.05	NA	NA	NA	NA	NA
JE3277	ASW MCA	12 m $CaCl_2$ + 0.6 m $Ca(NO_3)_2$	130	0.05	47	92	-37	-39	-39
JE3278	ASW MCA	12 m $CaCl_2$ + 0.6 m $Ca(NO_3)_2$	130	0.05	77	97	-35	-38	-39
JE3272	ASW MCA	12 m $CaCl_2$ + 1.8 m $Ca(NO_3)_2$	130	0.15	161	216	17	13	NA
JE3273	ASW MCA	12 m $CaCl_2$ + 1.8 m $Ca(NO_3)_2$	130	0.15	206	249	20	17	NA
JE3451	ASW MCA	12 m $CaCl_2$ + 6 m $Ca(NO_3)_2$	100	0.5	211[A]	297[A]	992	896	NA
JE3452	ASW MCA	12 m $CaCl_2$ + 6 m $Ca(NO_3)_2$	100	0.5	204[A]	286[A]	980	862	NA
JE3467	ASW MCA	12 m $CaCl_2$ + 6 m $Ca(NO_3)_2$	110	0.5	>1000	>1000	963	836	NA
JE3470	ASW MCA	12 m $CaCl_2$ + 6 m $Ca(NO_3)_2$	110	0.5	995	>1000	965	847	NA
JE3468	ASW MCA	12 m $CaCl_2$ + 6 m $Ca(NO_3)_2$	120	0.5	NA	NA	NA	NA	NA
JE3469	ASW MCA	12 m $CaCl_2$ + 6 m $Ca(NO_3)_2$	120	0.5	975	NA	940	693	NA
JE3279	ASW MCA	12 m $CaCl_2$ + 6 m $Ca(NO_3)_2$	130	0.5	NA	NA	NA	NA	NA
KE0386	ASW PCA	12 m $CaCl_2$ + 6 m $Ca(NO_3)_2$	130	0.5	940			800	NA
JE3453	ASW MCA	12 m $CaCl_2$ + 6 m $Ca(NO_3)_2$	130	0.5	937	NA	908	766	NA
JE3455	ASW MCA	12 m $CaCl_2$ + 6 m $Ca(NO_3)_2$	130	0.5	310	NA	868	192	NA
JE3454	ASW MCA	12 m $CaCl_2$ + 6 m $Ca(NO_3)_2$	150	0.5	837	982	817	696	NA
JE3456	ASW MCA	12 m $CaCl_2$ + 6 m $Ca(NO_3)_2$	150	0.5	772	986	501	252	NA
JE3461	ASW MCA	18 m $CaCl_2$	160	0	-93	-40	-174	-185	-184
JE3462	ASW MCA	18 m $CaCl_2$	160	0	-134	-73	-77	-83	NA
JE3274	ASW MCA	18 m $CaCl_2$ + 0.9 m $Ca(NO_3)_2$	160	0.05	93	123	14	11	11
JE3282	ASW MCA	18 m $CaCl_2$ + 0.9 m $Ca(NO_3)_2$	160	0.05	71	108	7	7	NA
JE3280	ASW MCA	18 m $CaCl_2$ + 2.7 m $Ca(NO_3)_2$	160	0.15	208	307	209	173	235
JE3283	ASW MCA	18 m $CaCl_2$ + 2.7 m $Ca(NO_3)_2$	160	0.15	163	280	79	67	65
JE3275	ASW MCA	18 m $CaCl_2$ + 9 m $Ca(NO_3)_2$	160	0.5	NA	NA	NA	NA	NA
JE3281	ASW MCA	18 m $CaCl_2$ + 9 m $Ca(NO_3)_2$	160	0.5	862	NA	825	698	NA

Table 2. Tested Conditions etc. (Continued)									
JE3300	ASW MCA	5 m $CaCl_2$ + 5 m $Ca(NO_3)_2$	100	1	NA	NA	NA	NA	NA
JE3252	ASW MCA	5.8 m NaCl + 2.4 m $NaNO_3$ + 18.2 m KNO_3	100	3.6	NA >600 [B]	NA >600 [B]	NA	485	NA
JE3253	ASW MCA	5.8 m NaCl + 2.4 m $NaNO_3$ + 18.2 m KNO_3	100	3.6	NA >600 [B]	NA >600 [B]	NA	478	NA
JE3254	ASW MCA	5.8 m NaCl + 2.4 m $NaNO_3$ + 18.2 m KNO_3	115	3.6	NA >600 [B]	NA >600 [B]	579	259	NA
JE3255	ASW MCA	5.8 m NaCl + 2.4 m $NaNO_3$ + 18.2 m KNO_3	115	3.6	NA >600 [B]	NA >600 [B]	592	159	NA
JE3298	ASW MCA	1.5 m $CaCl_2$ + 15 m $Ca(NO_3)_2$	125	10	NA >600 [B]	NA >600 [B]	NA	NA	NA
JE3299	ASW MCA	1.5 m $CaCl_2$ + 15 m $Ca(NO_3)_2$	125	10	869	999	835	709	NA
JE3292	ASW MCA	0.225 m $MgCl_2$ + 22.5 m $Ca(NO_3)_2$	145	100	NA >600 [B]	NA >600 [B]	NA	593	NA
JE3297	ASW MCA	0.225 m $MgCl_2$ + 22.5 m $Ca(NO_3)_2$	145	100	897	>1000	878	791	779
In the concentration of the electrolyte "m" stands for molal, which is moles of the solute (salt) per kilogram of solvent (water). NA = The potential is not available because the test was finished too soon or in the case of ERCO the intersection does not occur. A = Potential reached via an anodic peak, B = Max. Applied Potential of +600 mV SSC. ASW = as-welded. E_{corr} = is the free corroding potential after 24 h exposure in the given deaerated electrolyte. E20 = Is the potential in the forward scan of a cyclic polarization curve where the current density first reaches 20 μA/cm². ap = When the forward current reaches 20 μA/cm² via an anodic peak (the second number shows the potential for the last time the current reaches 20 μA/cm² in the forward scan). E200 = Is the potential in the forward scan of a cyclic polarization curve where the current density reaches 200 μA/cm². ER10 = Is the potential in the reverse polarization where the current density first reaches 10 μA/cm². ER1 = Is the potential in the reverse polarization where the current density first reaches 1 μA/cm². ERCO = is the cross-over potential. TR = Transpassivity, LC = Localized Corrosion (Includes pitting corrosion, crevice corrosion and border attack).									

Table 3. Constant Potential Testing Conditions

Specimen	Solution	$[NO_3^-]/[Cl^-]$	Temp. (°C)	Applied Potential (mV SSC)	Results after the tests
KE0375	10 m $CaCl_2$ + 5 m $Ca(NO_3)_2$	0.5	100	250	LC
KE0354	12 m $CaCl_2$ + 6 m $Ca(NO_3)_2$	0.5	130	750	No Corr.
KE0109	18 m $CaCl_2$ + 0.9 m $Ca(NO_3)_2$	0.05	155	50	LC
KE0353	18 m $CaCl_2$ + 9 m $Ca(NO_3)_2$	0.5	160	750	No LC
KE0509	5 m $CaCl_2$ + 5 m $Ca(NO_3)_2$	1	100	850	TP, No CC
KE0510	5 m $CaCl_2$ + 5 m $Ca(NO_3)_2$	1	100	900	
KE0512	0.225 m $MgCl_2$ + 22.5 m $Ca(NO_3)_2$	100	145	840	TP. No LC
KE0163	0.225 m $MgCl_2$ + 22.5 m $Ca(NO_3)_2$	100	145	850	TP. No CC
KE0511	0.225 m $MgCl_2$ + 22.5 m $Ca(NO_3)_2$	100	145	940	TP. No CC
CC = Crevice Corrosion, TP = Transpassivity, LC = Localized Corrosion					